Acta of Bioengineering and Biomechanics
Vol. 22, No. 1, 2020

Original paper
DOI: 10.37190/ABB-01479-2019-03

Influence of geometry and annealing temperature in argon atmosphere of TiO_2 nanotubes on their electrochemical properties

MARTA NYCZ[1]*, EWA PARADOWSKA[1], KATARZYNA ARKUSZ[1], DOROTA GENOWEFA PIJANOWSKA[2]

[1] Department of Biomedical Engineering, Faculty of Mechanical Engineering, University of Zielona Góra, Zielona Góra, Poland.
[2] Nalecz Institute of Biocybernetics and Biomedical Engineering, Polish Academy of Sciences, Warsaw, Poland.

Purpose: In this paper, electrochemical properties of the as-formed and thermally treated titanium dioxide (TiO_2) nanotubes with diameter in the range of 20–100 nm and height in the range of 100–1000 nm were presented. In addition, the effects of annealing temperature (450–550 °C) on the electrochemical characteristics of these structures, as well as the influence of diameter and height of TiO_2 nanotubes on these properties were examined. The results were referred to a compact TiO_2 layer (100 nm thick). *Methods*: The electrochemical test included open circuit potential, impedance spectroscopy and cyclic voltammetry measurements. The scanning electron microscope with energy dispersive spectroscopy analyser, x-ray photoelectron spectroscopy, and x-ray diffraction analysers were used for surface morphology characterisation as well as elemental, phase and chemical composition of TiO_2 layers. *Results*: It was found that nanotubes with the diameter of 50 and 75 nm (height of 1000 nm) annealed at 550 °C exhibit the lowest impedance and phase angle values. However, the voltammetric detection of potassium ferricyanide indicated that the closest to 1 I_{pc}/I_{pa} ratio were shown by nanotubes with a diameter of 50 and 75 nm annealed at 450 °C. *Conclusions*: On the basis of performed analysis, it can be stated that the TiO_2 layer with nanotubes of 50 nm in diameter and of 1000 nm in height, annealed in 450 °C may be indicated as the ones having the most favourable sensing and biosensing properties.

Key words: *titanium dioxide (TiO_2), titanium nanotubes (TNT), thermal modification, annealing*

1. Introduction

Electrochemical properties of materials have been examined to evaluate the possibility of their use for the detection of various types of compounds. A number of materials used as biosensor platforms, e.g., carbon materials, polymers, and gold, may be found in the literature. Nonetheless, the most widely used are metal oxides and metallic nanostructures. Titanium dioxide nanotubes (TNT) are very attractive electrode materials used as biosensor platforms possessing numerous beneficial properties in sensor technology: large specific surface area, high bioactivity, biocompatibility, thermal stability, corrosion resistance, ability to be colonised by bacteria, drug, enzyme and antibody immobilization [3], [8], [18]. These structures may be produced by: electrochemical oxidation, pattern technique, and hydrothermal processing. One of the cheapest and most frequently used methods is anodizing performed in an electrolyte solution with the assistance of electric field. The matrix parameters obtained using this method depend on many factors: concentration of fluoride ions and anodic potential, time of process, as well as electrolyte pH and type [2], [4], [16].

Ti/TNT properties are improved by thermal processing – annealing in different atmospheres which enables changing of TiO_2 in amorphous form (originally present in nanotubes) into crystalline form of

* Corresponding author: Marta Nycz, Department of Biomedical Engineering, Faculty of Mechanical Engineering, University of Zielona Góra, ul. prof. Z. Szafrana 4, 65-516 Zielona Góra, Poland. Phone: +48 789441696, e-mail: m.nycz@ibem.uz.zgora.pl
Received: October 17th, 2019
Accepted for publication: February 18th, 2020

rutile and/or anatase [8]. Crystallization of amorphous nanotubes to anatase takes place at temperature of about 300 °C, while rutile appears at about 450–550 °C [6], [26]. The rutile nucleation occurs first on the surface between the titanium substrate and the TiO_2 nanotubes, then on the top of the nanotubes, and finally, on their entire volume. It should be noted that the above temperature limits are contractual, because, according to Wang [22], the anatase crystallization or the anatase-rutile transformation temperature can occur within a wide temperature range of 400–1100 °C. It depends on the parameters of titanium foil, material preparation procedures, nanotube morphology (diameter, height), annealing atmosphere and dopants.

Morphology of TNT remains stable at the annealing temperature not exceeding 600 °C. Above this temperature, nanotubes begin to deform at the contact place with titanium foil. The collapse of the structure can be attributed to the increase of the rutile phase at the boundary between the barrier layer (electrically insulating layer separating titanium nanotubes) and the titanium substrate, where the metal is thermally anodized. The rutile phase is characterised by larger crystallites and growing during which they gradually make the nanotube walls merge with the collapse of the structure. At 700–800 °C, the nanotubular structure completely disappears leaving irregularly shaped grains, which is associated with high percentage of anatase to the rutile transformation and rapid growth of the rutile grains [22].

The most important advantage of annealing is that it causes the formation of oxygen vacancies, which results in improved TNT conductivity and thus, facilitates the transfer of charge that is attributed to the conversion of Ti^{4+} to Ti^{3+}. The electrical conductivity of TiO_{2-x} is proportional to the amount of oxygen vacancies. Studies show that annealing in argon generates more oxygen vacancies in TiO_2 than annealing in air, oxygen or nitrogen [6], [19]. Is the fact that deterioration of nanostructures at higher temperatures results in destabilization of their electrochemical characteristics.

At present, no results have been published on electrochemical characterisation of the TNT structure of fixed height and different diameters of the non-annealed and annealed in argon atmosphere nanotubes or vice versa of fixed diameter and different heights, as described in this paper. Most of the studies investigated the influence of annealing temperature [13], [22], compared the effects of one-step and two-step heat treatment [19], effects of composition of the solutions [1], concentration of fluoride ions, anodic potential and time [11], [14] on the electrochemical properties of the nanotubes.

In previous research of authors [2], the influence of annealing atmosphere on electrochemical properties of TiO_2 nanotubes was investigated, the best conductivity was characterised by argon-annealed substrates, which is why this atmosphere was used in the presented study. Additionally, previously, the influence of different temperatures as well as different heights and only the limited number of nanotube diameters were not taken into account, which supplements the current study.

The aim of this study was to investigate the influence of geometry and annealing temperature on titanium dioxide nanotubes electrochemical properties. The TNT structures were annealed at two temperatures (450 and 550 °C) in argon atmosphere. In addition, electrochemical studies of the compact TiO_2 layer were carried out as a reference. The amperometric detection of potassium ferricyanide was performed to calculate the electrochemical active surface area (EASA) of the TNT after thermal modification.

2. Materials and methods

2.1. Materials

Titanium (Ti) foil (purity of 99.7%, thickness of 0.25 mm), ethylene glycol (assay 99.8%), ammonium fluoride NH_4F, potassium ferricyanide $K_3[Fe(CN)_6]$, phosphate buffered saline (0.01 M PBS, 0.0027 M potassium chloride and 0.137 M sodium chloride, pH 7.4) and potassium chloride KCl were purchased from Sigma-Aldrich (USA) and used as supplied. All solutions were prepared from Milli-Q water.

2.2. TiO_2 nanotubes fabrication

The titanium foil was mechanically polished to a mirror using increasing grits of abrasive paper (70, 120, 600, 800, and 2000), followed by four different polishing alumina powders of decreasing particle size (mesh: 500, 600, 800, and 1200). The Ti foil were cut into 5 mm (width) × 15 mm (height) × 0.25 mm (thickness) and sonicated in acetone, distilled water and dried in nitrogen. The TiO_2 layers were prepared by electrochemical anodization of titanium foils in various concentrations of ethylene glycol solution with the presence or absence of ammonium fluoride, using Autolab PGSTAT302N (Metrohm). The 1-stage process was carried out using a two-electrode system

Table 1. Parameters of anodizing process of TiO_2 layers of different morphology formation (compact layer, nanotubular layer – TNT), where *h* stands for height of oxide laye and ∅ for diameter of titanium nanotubes

Type of TiO_2 layer	Potential [V]	Anodizing time [s]	Concentration of $C_2H_6O_2$ [%]	Concentration of NH_4F [%]
Compact (100 nm-thick)	4	7200	99	–
TNT (*h* = 100 nm, ∅ 20 nm)	4	7200	85	0.65
TNT (*h* = 1000 nm, ∅ 20 nm)	4	7200	90	
TNT (*h* = 1000 nm, ∅ 25 nm)	10	600	90	
TNT (*h* = 1000 nm, ∅ 50 nm)	17	3750	85	
TNT (*h* = 1000 nm, ∅ 75 nm)	30	900	90	
TNT (*h* = 1000 nm, ∅ 100 nm)	40	1100	85	

with a platinum sheet as a counter electrode and titanium foil as a working electrode, with the anodization surface of 5 mm × 5 mm × 0.25 mm. The oxide films were removed by mechanical detachment with using an adhesive tape. The TiO_2 layers of different morphology: compact oxide layer (100 nm thick), nanotubes with diameter of 20 nm and height of 100 nm and diameter of 20–100 nm and height of 1000 nm were obtained based on the anodizing parameters presented in Table 1. These parameters were selected on the basis of the developed mathematical model [10].

Scanning electron microscopy (FESEM, JEOL JSM-7600F) and energy-dispersive x-ray spectroscopy (EDS, Oxford INCA) were used to investigate the surface morphology and chemical composition.

2.3. Thermal modification

TNT layers were annealed in the AMP furnace (AMP Poland) in argon atmosphere at 450 and 550 °C for 2 h with the heating and cooling rate of 6 °C/min.

XRD were performed at Panalytical Empyrean diffractometer using Cu-K-α radiation at 40 kV and 40 mA (λ = 1.540508 Å).

XPS analysis were carried out in a PHI Versa Probe II Scanning XPS system using monochromatic Al-K-α (1486.6 eV) x-rays focused to a 100 µm spot and scanned over the area of 400 µm × 400 µm. The photoelectron take-off angle was 45° and the pass energy in the analyzer was set to 46.95 eV. Deconvolution of spectra was carried out using the PHI MultiPak software (v.9.9.0.8). Spectrum background was subtracted using the Shirley method.

2.5. Electrochemical measurements

The open circuit potential (OCP) tests and electrochemical impedance spectroscopy (EIS) scans for non-annealed and annealed samples were recorded using a standard three-electrode configuration with a compact titanium dioxide layer and titanium nanotubes of different morphology as the working electrode, standard silver chloride electrode ($E_{Ag/AgCl}$ = 0.222 V) as the reference electrode, and the platinum foil as the auxiliary electrode.

OCP measurements were carried out at room temperature (25 ± 2 °C) for 1800 s. EIS spectra were performed over a frequency range of $0.1 \div 10^5$ Hz with a signal amplitude of 10 mV. Cyclic voltammetry (CV) tests were carried out for potential ranging from –1 to 1 V vs. Ag/AgCl with the scan rate of 0.05 V/s. All experiments were performed in PBS solution (0.01 M, 20 ml, pH 7.4).

Electrochemical measurements in 1 mM $K_3[Fe(CN)_6]$ in 0.1 M KCl solution were carried out to calculate the electrochemical active surface area of TiO_2 surfaces after thermal modification at 450 and 550 °C in argon atmosphere for 2 hours. The Randles–Ševcik equation for a quasi-reversible system (at 298 K) is given in Eq. (1):

$$I_p^{\text{quasi}} = \pm(2.65 \times 10^5) n^{3/2} A C D^{1/2} v^{1/2}, \tag{1}$$

where I_p – peak current, n – number of electron transfer, A – electrochemical active surface area of the electrode, D – diffusion coefficient, v – scan rate and C – concentration of KCl solution. Potassium ferricyanide diffusion coefficient is equal to $7.6 \cdot 10^{-6}$ cm^2/s at 25 °C [23].

All measurements were repeated three times (for three samples n = 3). The results of electrochemical studies in the Bode representation show the curves for measuring the closest to the average value of the three samples (presented on all plots in the attached table of the average values with standard deviations) of non-annealed and annealed TiO_2 layers. The potentiostat/galvanostat model PGSTAT 302N from Autolab (Metrohm) was used for all tests.

3. Results

For the purpose of this study, a comparison of the electrochemical properties of a compact TiO_2 layer with nanotubular TiO_2 layer having the same height (100 nm) and as small as the possible diameter of nanotubes (20 nm) was carried out. Further analysis compared titanium nanotubes with the same diameter, i.e., 20 nm and varying height (100 or 1000 nm). Finally, the electrochemical properties of titanium nanotubes with varying diameter, range of 20–100 nm and the same height of 1000 nm were compared.

3.1. Characterisation of non-annealed TNT

The SEM micrographs (Fig. 1) show the structure of different morphology non-annealed TiO_2 layers of: compact TiO_2 layer (100 nm thick) and exemplary nanotubular structure – TiO_2 nanotubes with diameter of 100 nm and height of 1000 nm. The wall thickness of the nanotubes was evaluated in the range from 3 to 10 nm, depending on TNT diameter.

The diameters of titanium dioxide nanotubes increase with the increase of the anodization voltage (Table 1). Anodizing in organic solutions leads to the formation of nanotubes with smooth walls without any perforation. However, in the case of the compact TiO_2 layer (Fig. 1A), numerous surface irregularities and cracks are observed. SEM images of TNT (Fig. 1B) show opened from the top, closed at the bottom and vertically oriented regular nanotubes completely covering the titanium foil.

In Table 2, the OCP average values for non-annealed samples measured in 0.01 M PBS solution at room temperature during 1800 s are shown.

The Nyquist diagrams determined for the compact and nanotubular TiO_2 layers present fragments of wide, incomplete semicircles (Fig. 2A). It is also shown that the impedance modulus $|Z|$ depends on the height and diameter of TiO_2 nanotubes. Increase of their height from 100 to 1000 nm, for diameter of 20 nm causes decrease of impedance from 152589 ± 11419 to 36976 ± 7903 Ω. As the diameter of nanotubes increases, the sample resistance decreases (Table 3).

The phase angle values presented in Bode plots (Fig. 2B) recorded in the lowest frequencies (0.1 Hz) in the range of 52.6÷84.0° are related to homogeneity of the sample surface. The lowest porosity value of phase angle (84.0 ± 0.2°) was observed for the compact titanium oxide layer. The porosity of analyzed structure increases in the following order: compact layer (h = 100 nm), nanotubular layer (h = 100 nm, ∅ 20 nm), nanotubular layer (h = 1000 nm, ∅ 20 nm). For TNT samples with the same height of 1000 nm, diameter increase causes porosity decrease (Table 3).

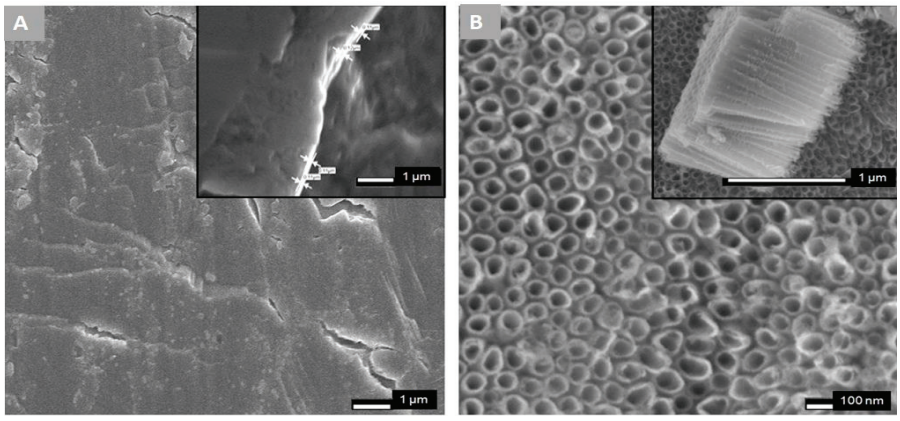

Fig. 1. SEM top-view and cross-sectional (on insets) images of:
(a) compact oxide layer (100 nm-thick); b) nanotubes with diameter of 100 nm and height of 1000 nm

Table 2. Average values of OCP and EDS results of compact and TNT layers

	Height of 100 nm		Height of 1000 nm				
TNT diameter [nm]	Compact layer	20	20	25	50	75	100
Ti [% wt.]	80.00	68.42	72.60	72.85	65.85	62.12	65.67
O [% wt.]	20.00	19.01	18.17	15.76	25.59	26.88	26.67
F [% wt.]	–	12.57	9.23	11.39	8.59	11.00	7.36
OCP [mV] vs. Ag/AgCl	–28 ± 5	–71 ± 7	–180 ± 23	–233 ± 26	–282 ± 27	–178 ± 40	–149 ± 24

Table 3. Average values of impedance parameters of compact and non-annealed TNT samples

	–*Z*phase [°]	–*ImZ* [Ω]	*ReZ* [Ω]	|*Z*| [Ω]
Compact (*h* = 100 nm)	84.0 ± 0.2	302559 ± 17633	31650 ± 2131	300328 ± 20126
TNT (*h* = 100 nm, ∅ 20 nm)	71.7 ± 1.4	144857 ± 10939	47856 ± 4895	152589 ± 11419
TNT (*h* = 1000 nm, ∅ 20 nm)	51.5 ± 4.9	28769 ± 6106	23078 ± 5964	36976 ± 7903
TNT (*h* = 1000 nm, ∅ 25 nm)	52.6 ± 4.1	26225 ± 8918	28969 ± 14289	39407 ± 15751
TNT (*h* = 1000 nm, ∅ 50 nm)	54.0 ± 2.1	9844 ± 853	7190 ± 824	12207 ± 1084
TNT (*h* = 1000 nm, ∅ 75 nm)	69.0 ± 1.2	4818 ± 472	1981 ± 439	5214 ± 607
TNT (*h* = 1000 nm, ∅ 100 nm)	72.3 ± 0.9	5570 ± 386	1804 ± 270	5857 ± 449

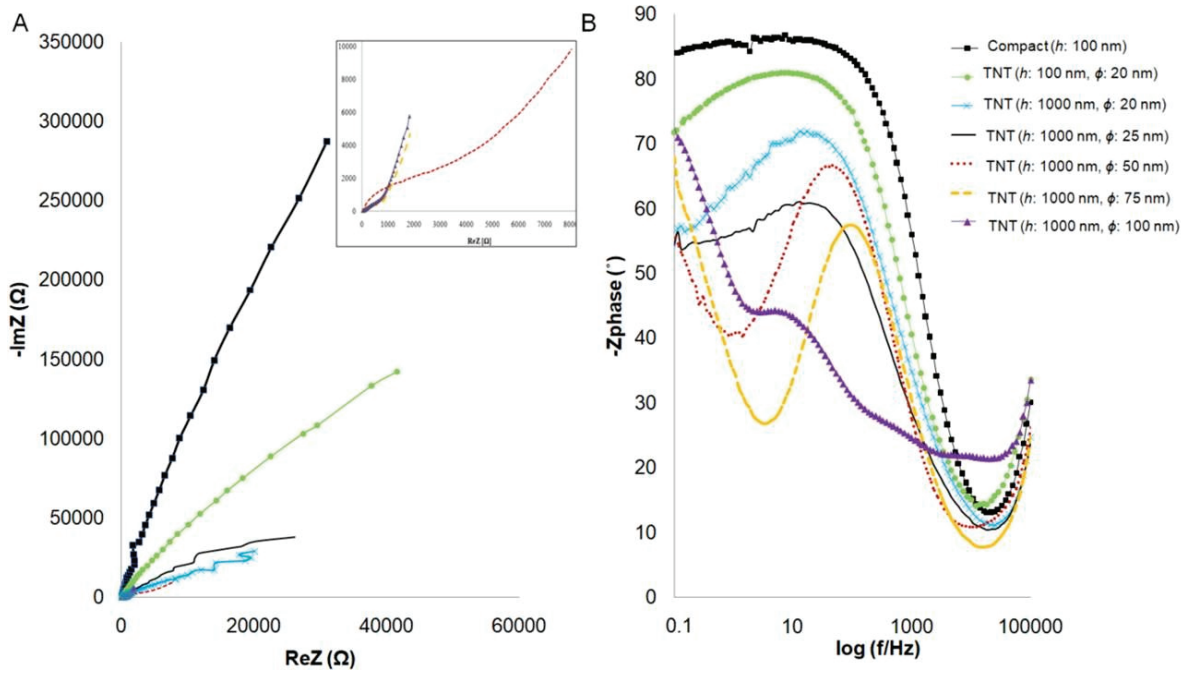

Fig. 2. (A) Nyquist and (B) Bode plots for non-annealed TiO_2 layers of different morphology

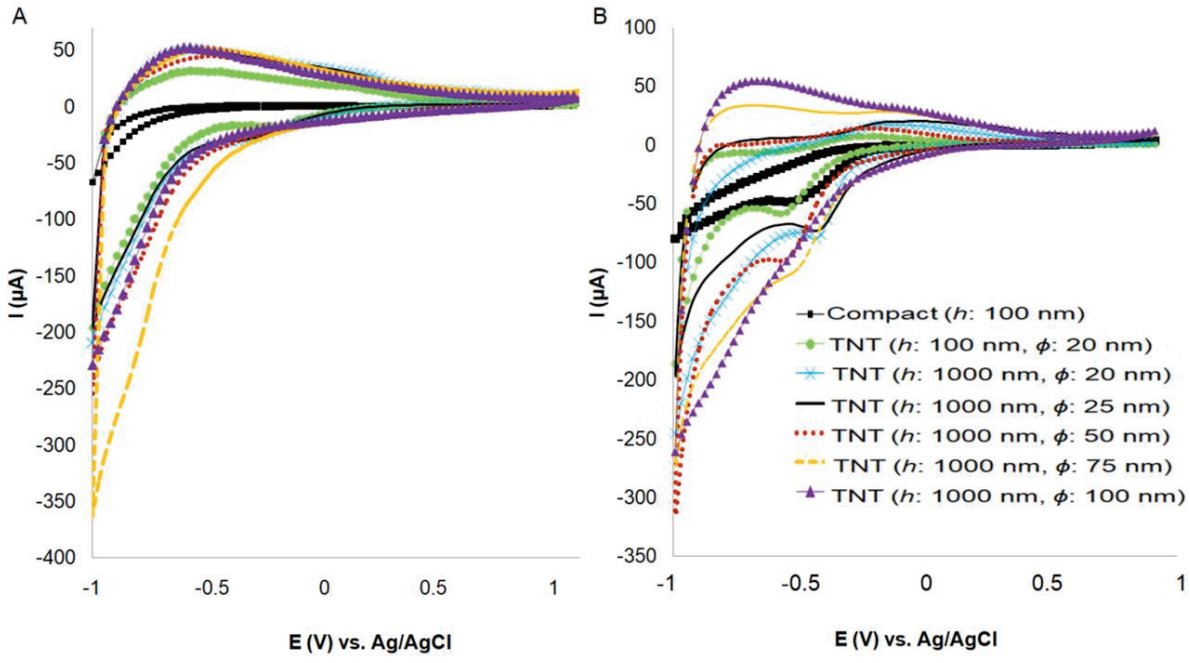

Fig. 3. Cyclic voltammograms of non-annealed TiO_2 layers of different morphology in:
(A) 0.01 M PBS and (B) 1 mM $K_3[Fe(CN)_6]$ in 0.1 M KCl

In Figure 3A, cyclic voltammograms for the analysed compact and nanotubular TiO_2 layer allowing for varying height and diameter of the nanotubes are shown. No oxidation and reduction peaks were observed. The biggest separation between cathodic and anodic half-waves, in particular for potential −0.7 V, were recorded for TNT with larger diameter (50–100 nm) and the smallest – for compact dioxide layer.

Potassium ferricyanide/potassium ferrocyanide (E_o = −0.36 V vs. hydrogen electrode) is one of the most commonly analysed redox couples in electrochemistry. Only for titanium nanotubes of diameter of 100 nm, no reduction and oxidation peak were observed. For the rest of analysed samples, the reduction peak centred in the range of −0.3÷—0.5 V and poorly formed anodic peak in the value of 0.1 V were observed. TNT with diameters of 25, 50 and 75 nm and height of 1000 nm showed the highest value of cathodic current peak. The biggest difference between anodic and cathodic curves was recorded for TNT with large diameter of 50–100 nm and the smallest for compact dioxide layer and TNT with diameter of 20 nm and height of 100 nm. Due to the non-reversible nature of the reaction for non-annealed samples, no electrochemical active surface area calculations were made.

3.2. Characterisation of annealed TNT

No damage on the TNT layers after annealing at 450 and at 550 °C for larger diameters (50, 75 nm) was observed, as shown in the exemplary microphotography of 50 nm diameter nanotubes (Fig. 4A). However, as a result of thermal treatment at 550 °C, the TNT of 25 nm diameter were damaged significantly causing change in their height from 1000 nm up to 300 nm (Fig. 4B) [5].

The OCP average values for TiO_2 nanotubes with varying diameters (25, 50, 75 nm) and 1000 nm height annealed at 450 °C and 550 °C for 2 hours in argon atmosphere, measured in 0.01 M PBS solution at room temperature during 1800 s are presented in Table 4. The increase in OCP values depends on the TiO_2 nanotubes diameter.

The EIS spectra of the annealed TNT layers with the height of 1000 nm and varying diameters (25, 50, 75 nm) are shown in Fig. 5 in Bode and Nyquist representations. The impedance values for the samples annealed at 450 °C decrease with the increase of TNT diameter (Table 5). Bode plots presented in Figs. 5C and D show that titanium nanotubes with the smallest

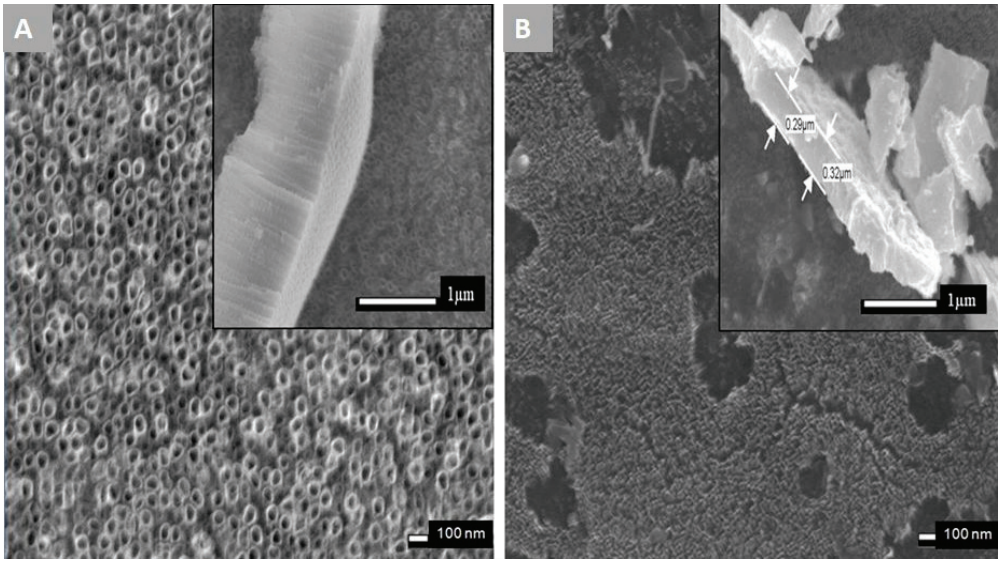

Fig. 4. SEM top-view and cross-sectional (on insets) images of titanium nanotubes of: (A) 50 nm and (B) 25 nm in diameter and 1000 nm in height after annealing at 550 °C

Table 4. Average values of OCP and EDS results of TNT after annealing at 450 °C and 550 °C

	Height 1000 nm					
Annealing temperature [°C]	450			550		
TNT diameter before annealing [nm]	25	50	75	25	50	75
TNT structure after annealing	Not changed			Destroyed	Not changed	
Ti [% wt.]	79.61	74.49	62.50	64.35	59.76	68.98
O [% wt.]	20.31	25.51	37.50	35.65	40.24	31.02
OCP [mV] vs. Ag/AgCl	−70 ± 11	35 ± 14	103 ± 18	−54 ± 13	14 ± 8	51 ± 18

Table 5. Average values of impedance parameters obtained for annealed TNT samples

Annealing temperature [°C]	TNT layer (h = 1000 nm)	–Zphase [°]	$-ImZ$ [Ω]	ReZ [Ω]	$\|Z\|$ [Ω]
450	∅ 25 nm	68.2 ± 4.7	42157 ± 4819	18899 ± 4088	42612 ± 1396
	∅ 50 nm	77.0 ± 0.6	8574 ± 581	1978 ± 65	8800 ± 576
	∅ 75 nm	72.4 ± 5.2	7019 ± 695	2228 ± 680	7386 ± 686
550	∅ 25 nm	56.1 ± 5.5	21759 ± 2796	14631 ± 2617	26310 ± 2811
	∅ 50 nm	79.6 ± 2.3	4039 ± 436	746 ± 213	4109 ± 459
	∅ 75 nm	78.0 ± 1.5	6629 ± 902	1372 ± 112	6770 ± 893

diameter (25 nm) are characterised by the highest value of phase angle. In the case of the TiO_2 nanotubes annealed in 550 °C, the highest value of impedance (26310 ± 2811 Ω) was also observed for TNT of the smallest diameter – 25 nm.

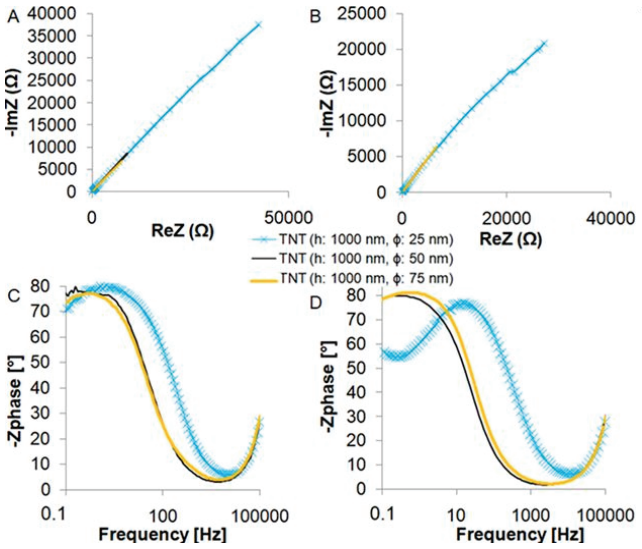

Fig. 5. Nyquist and Bode plots of TNT of 25–75 nm diameter and 1000 nm in height annealed in (A), (C) 450 °C and (B), (D) 550 °C

The electrochemical properties of titanium dioxide nanotubes of various diameters (25, 50, 75 nm) annealed at two temperatures (450 and 550 °C) in argon atmosphere for 2 hours were investigated by means of cyclic voltammetry in 0.01 M PBS (20 ml, pH 7.4) as an electrolyte in a potential range of −1 V to 1 V versus Ag/AgCl at a scan rate of 0.05 V/s (Fig. 6). The anodic and cathodic current values increase with the increasing nanotube diameter.

The voltammetric detection of $K_3[Fe(CN)_6]$ for the annealed in argon atmosphere TNT are presented in Fig 7. Unequal oxidation and reduction peak current suggest a quasi-reversible electrochemical reaction. For example, in the case of TNT of 75 nm diameter annealed at 550°C, the height of the anodic peak is equal to 7.34 µA and the cathodic 4.34 µA. The peak current increases as the annealing temperature and the nanotube diameter increases. For the nanotubes after the annealing process at 450 °C, small oxidation/reduction peaks centred at ~0.4 V/~0 V for TNT of 50 nm diameter, and ~0.40 V/~−0.02 V – for 75 nm in diameter (i.e., peak separation: ~0.40 V and ~0.42 V, respectively) were observed. For the titanium nanotubes with 50 nm and 75 nm in diame-

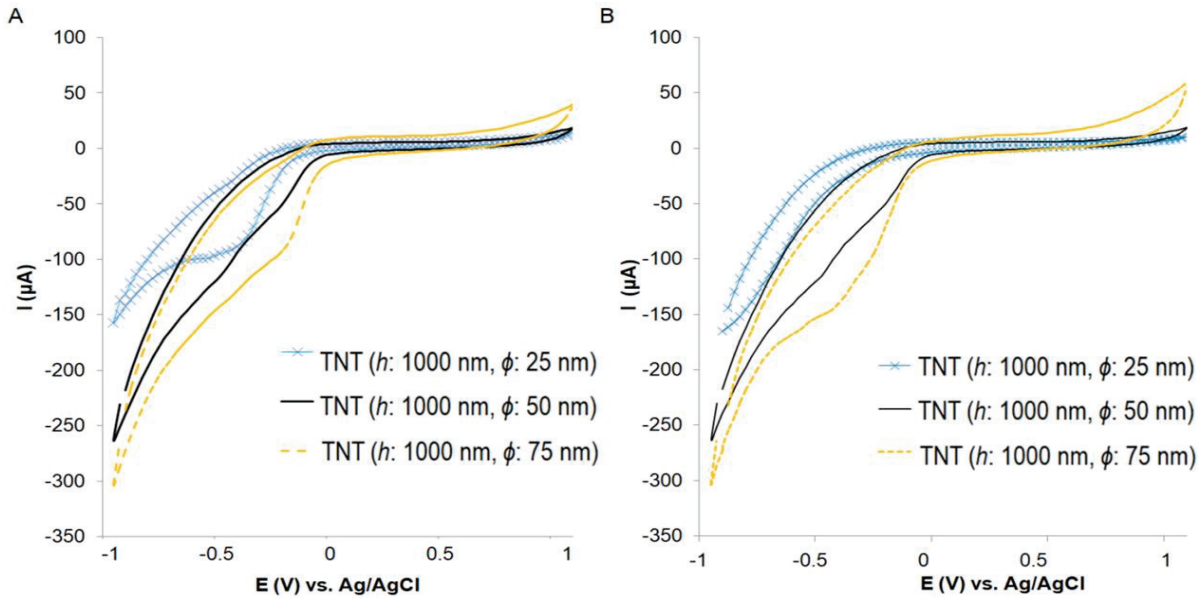

Fig. 6. Cyclic voltammograms of TNT of 25–75 nm diameter and 1000 nm height annealed in (A) 450 °C and (B) 550 °C

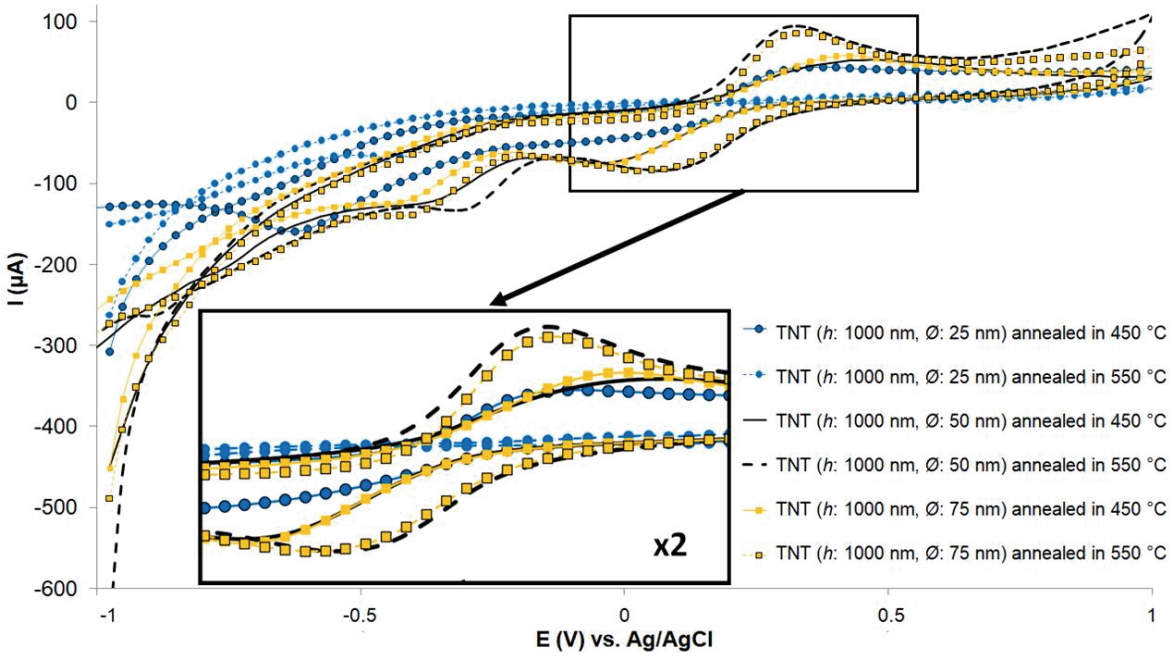

Fig. 7. Cyclic voltammograms of TNT of 25–75 nm in diameter and 1000 nm in height annealed in 450 °C and 550 °C

Table 6. Average values of the cathodic (I_{pc}), anodic (I_{pa}) current peaks and electrochemical active surface area ($EASA_{pc}$ – determined from I_{pc}, $EASA_{pa}$ – from I_{pa}) for TNT of 1000 nm height and 25–75 nm in diameter after annealing in argon at 450 and 550 °C

Annealing temperature [°C]	TNT layer (h = 1000 nm)	I_{pc} [$\times 10^{-5}$ A]	I_{pa} [$\times 10^{-5}$ A]	I_{pc}/I_{pa}	$EASA_{pc}$ [cm^2]	$EASA_{pa}$ [cm^2]
450	∅ 25 nm	1.12 ± 0.02	2.70 ± 0.11	0.41 ± 0.18	0.61 ± 0.01	1.48 ± 0.06
	∅ 50 nm	2.78 ± 0.03	3.45 ± 0.23	0.81 ± 0.13	1.52 ± 0.02	1.89 ± 0.13
	∅ 75 nm	3.75 ± 0.04	3.94 ± 0.18	0.95 ± 0.22	2.05 ± 0.02	2.16 ± 0.10
550	∅ 25 nm	1.63 ± 0.47	–	–	0.89 ± 0.26	–
	∅ 50 nm	4.06 ± 0.15	6.98 ± 0.12	0.58 ± 1.25	2.22 ± 0.08	3.82 ± 0.07
	∅ 75 nm	4.34 ± 0.17	7.34 ± 0.20	0.59 ± 0.85	2.37 ± 0.09	4.02 ± 0.11

ter annealed at 550 °C, well-defined oxidation/reduction peaks potential separation for these samples was approximately ~0.40 V and ~0.42 V. Increasing the annealed temperatures does not affect anodic and cathodic peak separation. The smallest peak separation for TNT of 50 nm diameter, in the case of voltammetric detection of potassium ferricyanide, is associated with the higher electrical conductivity.

The electrochemical active surface areas of the TNT nanotubes after thermal modification in argon atmosphere were determined using cyclic voltammetry according to the Randles–Ševcik equation for the quasi-reversible redox couples (1), based on experiments performed in 1 mM $K_3Fe(CN)_6$ in 0.1 M KCl solution. The electrochemical active surface area values presented in Table 6 were calculated by determining the heights of current peaks (I_{pc} and I_{pa}).

3.3. XRD and XPS characterisation of TiO_2 nanotubes of 50 nm in diameter and 1000 nm in height before and after annealing

The X-ray diffraction analysis results presented in Fig. 8 confirmed the occurrence of titanium and amorphous titanium dioxide in as-formed samples. Both annealed samples contained anatase in a high proportion, the sample annealed at 550 °C contained a greater amount of rutile than the sample annealed at 450 °C. These results confirm that the transformation of anatase to rutile appears at about 450–550 °C and that increasing the heat treatment temperature results in increasing the rutile content [6], [26].

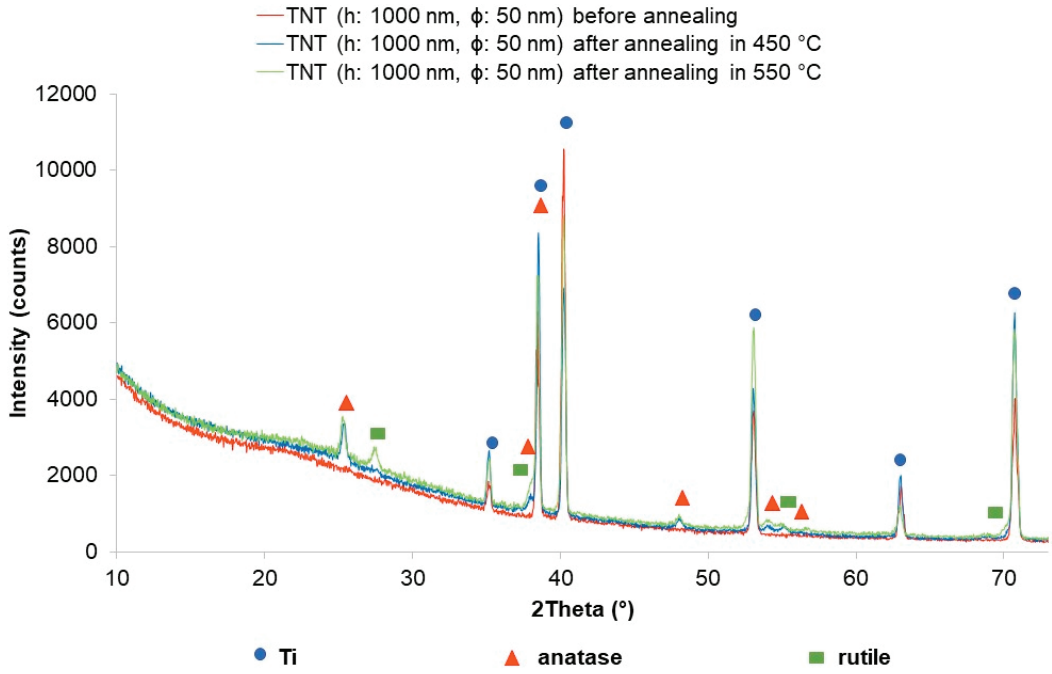

Fig. 8. XRD patterns of as-formed and annealed titanium dioxide nanotubes of 50 nm in diameter and 1000 nm in height

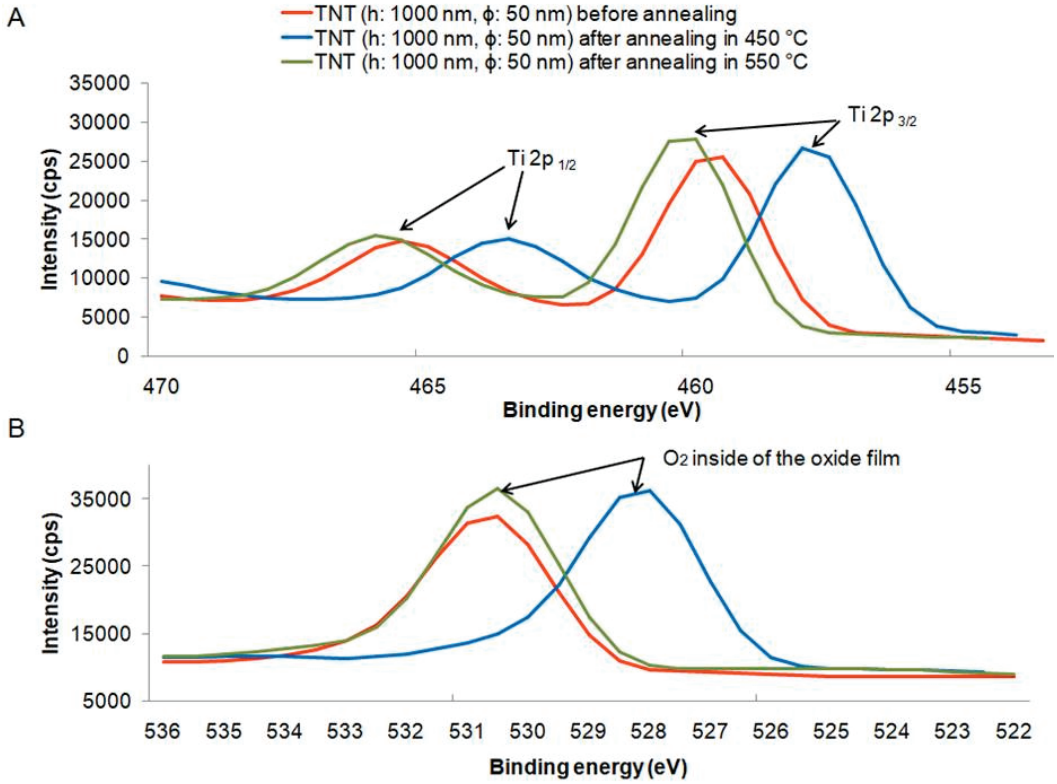

Fig. 9. XPS patterns of as-formed and annealed titanium dioxide nanotubes of 50 nm in diameter and 1000 nm in height: (A) Ti 2*p* spectra, (B) O 1*s* spectra

The results of the XPS analysis of the TNT before and after thermal modification are shown in Fig. 9. TiO_2 and Ti_2O_3 were found on the surface of analysed samples, both thermal modified and non-modified TNT layer. The standard binding energy of Ti 2*p*3/2 in TiO_2 for Ti^{3+} is usually located at 457.7 eV and for Ti^{4+} is at 459.5 eV [4]. The O 1*s* binding energy for TiO_2 is 530.2 eV [24]. The analysis of the XPS depth profile of TNT layers before and after thermal modification indicates higher amount of oxygen absorbed

inside of the oxide film rather than on its surface (a poorly formed peak not marked on the graph). Thermal modification of TNTs results in the occurrence of the lack of oxygen on the surface, which proves its deficiency, the presence of oxygen vacancies and results in improved TNT electrical conductivity. Thermal modification causes increases in the peak height compared to unmodified samples. For samples annealed in 450 °C, the shift to lower binding energies of O 1*s* and Ti 2*p* spectra was observed. A shift to lower binding energy of Ti^{3+} indicates that electrons bound to the oxygen and titanium ions migrated to the oxygen vacancies; with the latter serving as electron traps. The shift in O 1*s* spectra can be attributed to the transfer of electrons to the neighbouring oxygen vacancies [24].

4. Discussion

4.1. Characterisation of non-annealed TNT

The OCP values for as-formed TiO_2 layer increase with the increase of nanotube diameter from 50–100 nm (Table 2). For samples with the height of 1000 nm, the open circuit potential graph shows (data not shown) small current oscillations probably as a result of release of fluoride ions from the interior of the nanotubes. Since TNT of 20, 25 and 75 nm in diameter and 1000 nm are deposited from anodizing solution containing higher concentration of ethylene glycol (90%) (Table 1), the higher viscosity of these solutions may result in difficulties with release of fluoride ions from nanotubular structures. The Ti/O ratio is superior to the stoichiometric TiO_2, which is due to the presence of another type of oxide: Ti_2O_3, which was also confirmed by previous studies of the authors [2]. Oxygen can also be adsorbed from OH^- groups present in the electrolytes [8]. No relationship between the diameter and/or height of nanotubes and the Ti/O ratio was observed.

The wide, incomplete semicircles showed on Nyquist diagrams for the compact and nanotube TiO_2 as-formed layers (Fig. 2A) are characteristic of thin oxide layers [7]. The highest resistive character, indicating the worst electrical conductivity, was observed for the compact dioxide layer (300328 ± 20126 Ω) and TNT with diameter of 20 nm and height of 100 nm (152589 ± 11419 Ω) (Table 3). On the other hand, the lowest |Z| values were observed for TNT of height of 1000 nm and diameter of 75 and 100 nm (Table 3). According to the standard deviation of the impedance modulus, values are close for these samples.

The impedance spectrum (Bode plot) recorded for compact TiO_2 layer has one time constant with frequency about 300 Hz, which confirms the presence of an oxide layer on the Ti base (Fig. 2B). In the case of TNT, two time constants are observed, which may be caused by the presence of dissolving oxide layer (with the fluoride ions) between nanotubes and Ti. For samples with the same diameter (20 nm), the first time constant at the frequency of 50 Hz was observed and the second time constant – at the lowest frequencies. The height affects their heterogeneity: the increase in TNT height causes the phase angle increase. In the case of titanium nanotubes of equal height their diameter affects the shift of the first time constant to the higher frequencies. The TNT diameter increase reduces the phase angle value (Table 3). For the nanotubes with dimensions of 100 nm and 1000 nm in height the time constant describing the TNT layer is not unequivocally defined as for other samples.

Neither anodic (Ti^{3+} to Ti^{4+} conversion) nor cathodic peaks related to Ti^{4+} to Ti^{3+} reduction and the H^+ release reaction were observed on the voltammograms for as-formed TiO_2 layers (Fig. 3A), which, according to Macak et al. [12], is characteristic of non-annealed TNT for which the reaction is relatively sluggish or hard to observe at all. The greater the separation between cathodic and anodic half-waves, the higher the conductivity. Samples of 75 nm in diameter and 1000 nm in height showed the highest conductivity (Fig. 3A). The separation between anodic and cathodic half-waves depends on the height of nanotubes. TNT of 100 nm height and 20 nm diameter have smaller current separation than samples of the same diameter but 1000 nm in height (Fig. 3A). The increase of nanotube diameter and height causes the increase of surface electrical conductivity.

In the case of voltammetric detection of potassium ferricyanide, a clearly visible cathode peak and a poorly defined anode peak were observed (Fig. 3B). It proves non-reversible nature of the reaction at TiO_2-TNT non-annealed electrodes [25]. This is characteristic for less conductive electrodes for which it is difficult for the electroactive molecules to lose electrons on the electrode surface, so the oxidation current density is lower than the reduction current density.

In conclusion, non-modified TiO_2 platforms varying in type structure (nanotubular and compact layer), the best conductivity characteristics show the TNT samples with the height of 1000 nm and diameters of

25, 50, 75 and 100 nm. However, the difference in impedance module between nanotubes with a diameter of 75 and 100 nm is minimal (Table 3). Among these samples, the highest cathodic peak current for detection potassium ferricyanide was observed for nanotubes with diameter of TNT 25, 50 and 75 nm. For the above-mentioned reasons, TNT samples of 1000 nm height and the diameter between 25–75 nm were chosen for further analysis related to the influence of thermal modification on electrochemical performance.

4.2. Characterisation of annealed TNT

The thermal modification of samples resulted in OCP values increase (Table 4), and thus, the corrosion resistance increase, which is consistent with the results presented by Mazarea et al. [13], Xiao et al. [14] and Yu et al. [25]. For TNT with the diameter of 50 nm and 75 nm, the OCP values were shifted to positive, which is attributed to the reduction of the amount of adsorbed water and OH^- groups on the surface of the nanotubes as a result of the annealing.

As it is well known, negatively charged protein molecules are easily attracted to the positively-charged matrix, which might be used in construction of platform for biosensor [21]. As demonstrated in previous studies, biomolecules can adsorb to even very smooth surfaces [17]. No current oscillations were observed on the OCP curves (data not shown), which can be explained by removal of the fluoride ions from the TNT samples due to the annealing at 400 °C and above, which was confirmed by Zhu et al. [26] and in previous studies of the authors of paper [2]. The Ti/O ratio is superior to the stoichiometric TiO_2, which is due to the presence of oxygen vacancies [2], [19]. No relationship between the diameter of nanotubes and the Ti/O ratio was observed.

In the case of annealing at 450 °C, the highest value of impedance modulus (42612 ± 1396 Ω) was observed for TNT with 25 nm in diameter, whereas the lowest (7386 ± 686 Ω) – for 75 nm in diameter (Table 5). These results are confirmed by studies Li et al. [11], in which the nanotubes with the smallest diameter (16 nm) had the largest impedance value. According to the standard deviation for nanotubes of 50 nm and 75 nm in diameter, the $|Z|$ values were similar. In the case of annealing at 550 °C, the highest resistivity of TNT with 25 nm in diameter is caused by the damage of TNT layer during the annealing process. The best electrical conductivity and the lowest phase angle were noted for nanotubes with 50 nm in diameter.

Heat treatment reduces the phase angle, hence, the heterogeneity of samples decreases. The impedance spectra recorded for the samples annealed at both temperatures display two phase angle peaks, where the low-frequency angle peak is attributed to the barrier film (between the Ti foil and the nanotubes) and the high-frequency angle peak is related to TNT itself [1], [7], [11], [14]. The differences in ReZ of TNT annealed in varying temperatures in the same atmosphere can be explained by non-linear I/V characteristics of polycrystalline TiO_2 nanotubes [20]. This mechanism, considering a barrier formed between the grains and the fluctuation induced tunnelling conductance, strongly depends on the anatase content in analysed samples, which in turn depends on annealing temperatures and morphology of TNT (i.e. diameter and height). The microscopic analysis also confirmed the influence of scattering of anatase content on the electrical properties of TNT samples [15]. According to Wang et al. [19] and Salari et al.'s [22] studies, the titanium dioxide nanotubes, which are mostly composed of rutile phase, exhibit higher conductivity and easier charge transfer. This can be attributed mainly to the conversion of Ti^{4+} to Ti^{3+}, higher annealing temperature, and greater content of the rutile phase in the modified structure. The results obtained by the authors are consistent with data obtained by others [19], [22], as the samples annealed at 550 °C, and, therefore, containing more rutile phase (Fig. 8), are characterised by a lower impedance modulus than samples annealed at 450 °C (Table 5). The analysis of the XPS (Fig. 9) depth profile of TNT layers before and after thermal modification indicates higher amount of oxygen absorbed inside. Thermal modification process results in improved TNT electrical conductivity.

The best electron transport properties of the samples annealed at 450 °C, due to the I_{pc}/I_{pa} ratio close to 1, are shown by titanium nanotubes with a diameter of 50 and 75 nm (Table 6). The reversible electrochemical behaviour observed with the redox couples shows the highest conductivity [21]. The highest disparity in peak currents (the cathodic peak is almost twice as high as the anodic) presents TiO_2 nanotubes with a diameter of 25 nm. Raising the annealing temperature results in decrease in nanotube conductivity – decreases the I_{pc}/I_{pa} ratio (significant disproportion in the heights of current peak) (Tabe 6). For TiO_2 nanotubes with 25 nm in diameter, annealed at 550 °C, only the cathodic peak was observed (Fig. 7). The same behaviour is characteristic for non-annealed nanotubes, so it can be stated that the distraction of TNT layer caused by thermal treatment results in the return of the original nanotube properties (as-formed).

The reversible electrochemical behaviour was extremely important for the construction of electrochemically active surfaces. Increase of the annealing temperature results in the increase of EASA values for nanotubes of 50 nm and 75 nm in diameter and 1000 nm in height (Table 6). As suggested in [9], the high EASA values mean that active electrode surface consists of a large conducting regions.

5. Conclusions

This paper presents comparison of electrochemical properties of varying type of titanium dioxide, i.e., compact and nanotubular layers. In addition, the influence of the morphology of titanium nanotubes (diameter and height) and annealing temperature in argon atmosphere on electrochemical behaviour was examined.

Comparison of compact and nanotubular TiO_2 layer having the same height, i.e., 100 nm indicates more negative corrosion potential, higher impedance modulus, lower difference between anodic and cathodic curves of TNT, which is caused by the release of fluoride ions after TNT formation process and higher specific surface area that provides a larger amount of OH^- on the TNT surface.

Increasing the height of TNT causes the decrease of OCP and impedance modulus values, increase of heterogeneity of TNT and the faradaic current separation. Performed analysis has also let to determine the relationship between the diameter of TNT having the same height (taken as 1000 nm) and its electrochemical response. The increase in diameter generally results in the increase of OCP values, surface heterogeneity and current recorded using cyclic voltammetry, as well as a decrease in the impedance modulus (both real and imaginary parts of impedance). It should be pointed out that this relationship often exclude TNT with 50 nm diameter.

Thermal modification by annealing in argon at varying temperatures (450 °C and 550 °C) were performed to improve the conductivity of the TNT layer. Annealing at 550 °C caused damage and collapse of the nanotubular structures for samples of 25 nm in diameter and 1000 nm in height. With the increase of nanotube diameter, the resistance to temperature-damaging effect increases. The OCP values increase after annealing, and for larger diameters (50, 75 nm) show positive values, indicating higher corrosion resistance of these samples. Heat treatment reduces the value of impedance modulus for TNT samples with smaller diameters (25 nm and 50 nm): the higher annealing temperature, the lower impedance modulus value. For nanotubes of the diameter of 75 nm, no significant changes in impedance were observed. Under the influence of temperature, the decrease of phase angle values was noticed as a result of reduction of the heterogeneity of the samples. TNT with the diameter of 50 nm and height of 1000 nm, annealed at 550 °C. show the lowest impedance modulus and phase angle values. Based on the EIS measurements, it was stated that samples annealed at higher temperatures (550 °C) were characterised by the higher conductivity than samples annealed at 450 °C. The performed electrochemical measurements clearly confirm that thermal modification results in improved electrochemical properties of the samples.

Cyclic voltammetry scans performed in PBS solution show that with the increasing diameter of annealed TNT, the separation between anodic and cathodic half-waves increase. Voltammetric detection of potassium ferrocyanide for as-formed samples showed only cathodic peaks, indicating the non-reversible nature of this process. The highest cathodic peaks were recorded for the untreated TNT with the height of 1000 nm and diameter of 50–100 nm. In the case of annealed TNT, the cathodic and anodic peaks were observed. Their height increased along with the increase of the annealing temperature. However, unequal oxidation and reduction of peaks current suggested a quasi-reversible electrochemical reaction.

On the basis of performed analysis, it can be stated that the TNT layer with diameter 50 nm and height 1000 nm, annealed in 450 °C, may be indicated as having the most favourable sensing and biosensing properties. This structure is characterised by OCP values close to zero, one of the smallest impedance modulus and high I_{pa}/I_{pc} ratio for potassium ferricyanide, which confirms good conductivity and good adsorption properties of this structure. Moreover, titanium nanotubes annealed at this temperature have more anatase structures that promote the adsorption of biological elements.

Acknowledgements

This research was funded by National Science Centre (Poland), grant number 2017/27/N/ST7/01702 and by grant financed from the Research and Development Fund of the Deputy Rector for Science and International Cooperation of the University of Zielona Góra.

References

[1] AINOUCHEA L., HAMADOUA L., KADRIA A., BENBRAHIMA N., BRADAI D., *Interfacial barrier layer properties of three generations of TiO_2 nanotube arrays*, Electrochim. Acta, 2014, 133, 597–609.

[2] ARKUSZ K., KRASICKA-CYDZIK E., *The effect of phosphates and fluorides included in TiO_2 nanotube layers on the performance of hydrogen peroxide detection*, Arch. Metall. Mater., 2018, 63, 761–768.

[3] ARKUSZ K., NYCZ M., PARADOWSKA E., *Electrochemical Evaluation of the Compact and Nanotubular Oxide Layer Destruction under Ex Vivo Ti6Al4V ELI Transpedicular Screw Implantation*, Materials, 2020, 13, 176.

[4] ARKUSZ K., PARADOWSKA E., NYCZ M., KRASICKA-CYDZIK E., *Influence of thermal modification and morphology of TiO_2 nanotubes on their electrochemical properties for biosensors applications*, J. Nanosci. Nanotechnol., 2018, 18, 3713–3721.

[5] BULBUL E., AKSAKAL B., *Synthesizing and characterization of nano-graphene oxide-reinforced hydroxyapatite coatingson laser treated Ti6Al4V surfaces*, Acta Bioeng. Biomech., 2017, 19, 171–180.

[6] GHICOV A., TSUCHIYA H., MACAK J.M., SCHMUKI P., *Annealing effects on the photoresponse of TiO_2 nanotubes*, Phys. Stat. Sol. A, 2006, 203, 28–30.

[7] GOODARZI S., MOZTARZADEH F., NEZAFATI N., OMIDVAR H., *Titanium dioxide nanotube arrays: A novel approach into periodontal tissue regeneration on the surface of titanium implants*, Adv. Mater. Lett., 2016, 7, 209–215.

[8] JAROSZ M., PAWLIK A., SZUWARZYŃSKI M., JASKUŁA M., SULKA G.D., *Nanoporous anodic titanium dioxide layers as potential drug delivery systems: Drug release kinetics and mechanism*, Coll. Surf. B. Biointer., 2016, 143, 447–454.

[9] JE-HWANG R., GI-JA L., WAN-SUN K., HAN-EOL L., MALLORY M., KYU-CHANG P. et al., *All-carbon electrode consisting of carbon nanotubes on graphite foil for flexible electrochemical applications*, Materials, 2014, 7, 1975–1983.

[10] KRASICKA-CYDZIK E., ARKUSZ K., KACZMAREK-PAWELSKA A., *A mathematical model for selection of formation parameters of TiO_2 nanotube by anodizing*, Eng. Biomat., 2012, 15, 34–40.

[11] LI D.G., CHEN D.R., WANG J.D., LIANG P., *Effect of acid solution fluoride ions anodic potential and time on the microstructure and electronic properties of self-ordered TiO_2 nanotube arrays*, Electrochim. Acta, 2016, 207, 152–163.

[12] MACAK J.M., TSUCHIYA H., GHICOV A., YASUDA K., HAHN R., BAUER S. et al., *TiO_2 nanotubes: Self-organized electrochemical formation properties and applications*, Curr. Opin. Solid State M., 2007, 11, 3–18.

[13] MAZAREA A., TOTEAB G., BURNEIC C., SCHMUKI P., DEMETRESCUD I., IONITAD D., *Corrosion antibacterial activity and haemocompatibility of TiO_2 nanotubes as a function of their annealing temperature*, Corros. Sci., 2016, 103, 215–222.

[14] MUNIRATHINAM B., NEELAKANTAN L., *Titania nanotubes from weak organic acid electrolyte: Fabrication characterization and oxide film properties*, Mat. Sci. Eng. C-Mater., 2015, 49, 567–578.

[15] MUÑOZ A.G., *Semiconducting properties of self-organized TiO_2 nanotubes*, Electrochim. Acta, 2017, 52, 4167–4176.

[16] NYCZ M., ARKUSZ K., PIJANOWSKA D.G., *Influence of the silver nanoparticles (AgNPs) formation conditions onto titanium dioxide (TiO_2) Nanotubes based electrodes on their impedimetric response*, Nanomaterials, 2019, 9, 1072.

[17] NYCZ M., PARADOWSKA E., ARKUSZ K., KUDLIŃSKI B., KRASICKA-CYDZIK E., *Surface analysis of long-term hemodialysis catheters made of carbothane (Poly(carbonate)urethane) before and after implantation in the patients' bodies*, Acta Bioeng. Biomech., 2018, 20, 47–53.

[18] PARADOWSKA E., ARKUSZ K., PIJANOWSKA D.G., *The Influence of the Parameters of a Gold Nanoparticle Deposition Method on Titanium Dioxide Nanotubes, Their Electrochemical Response, and Protein Adsorption*, Biosensors, 2019, 9 (4), 138.

[19] SALARI M., KONSTANTINOV K., LIU H.K., *Enhancement of the capacitance in TiO_2 nanotubes through controlled introduction of oxygen vacancies*, J. Mater. Chem., 2011, 21, 5128–5133.

[20] STILLER M., ESQUINAZI P., SO S., HWANG I., SCHMUKI P., BÖTTNER J. et al., *Electrical transport properties of polycrystalline and amorphous TiO_2 single nanotubes*, Nano--Structures and Nano-Objects, 2017, 10, 51–56.

[21] WANG J., LIN Z., *Anodic formation of ordered TiO_2 nanotube arrays: effects of electrolyte temperature and anodization potential*, J. Phys. Chem. C, 2009, 113, 4026–4030.

[22] WANG Y., LIU S., HUANG K., FANG D., ZHUANG S., *Electrochemical properties of freestanding TiO_2 nanotube membranes annealed in Ar for lithium anode material*, J. Solid. State. Electr., 2012, 16, 723–729.

[23] YAN Y., WU L., GUO Q., HUANG S., *A novel catechol electrochemical sensor based on cobalt hexacyanoferrate/(CoHCF)/Au/SBA-15*, J. Anal. Bioanal. Tech., 2015, 6, 290.

[24] YEW R., KARUTURI S.K., LIU J., TAN H.H., WU Y., JAGADISH C., *Exploiting defects in TiO_2 inverse opal for enhanced photoelectrochemical water splitting*, Opt. Express, 2019, 27, 761–773.

[25] YU W., QIU J., XU L., ZHANG F., *Corrosion behaviors of TiO_2 nanotube layers on titanium in Hank's solution*, Biomed. Mater., 2009, 4, 065012.

[26] ZHU K., NEALE N.R., HALVERSON A.F., KIM J.Y., FRANK A.J., *Effects of annealing temperature on the charge-collection and light-harvesting properties of TiO_2 nanotube-based dye-sensitized solar cells*, J. Phys. Chem. C, 2010, 114, 13433–13441.